

# Learning to Think on Hypergraph: HyperCoT for Structure-Guided N-ary Knowledge Graph Completion

Anonymous ACL submission

## Abstract

$N$ -ary knowledge graph completion (KGC) aims to infer missing components in facts with multiple entities under distinct semantic roles, commonly formulated as a knowledge hypergraph link prediction task. Most embedding-based approaches score individual hyperedges relying on enriched structural representations, but overlook intermediate propagation states containing complementary local and global structural evidence. Despite their capability to generate chain-of-thought (CoT) representations for the classical KGC task, large language models (LLMs) struggle with hypergraph structure involving multiple facts, while current hypergraph QA methods only provide LLMs with a single query signal rather than path-level evidence. These limitations hinder the transferability of existing methods, especially those leveraging LLMs, to solve knowledge hypergraph link prediction problem. To bridge this gap, we propose **HyperCoT**, a structure-aware approach that models multi-hop structural reasoning as a *depth-sensitive progressive evidence accumulation* process. It constructs a *Graphical Chain-of-Thought (Graph-CoT)* by aggregating role-aware hyperedge states along strongly correlated reasoning paths, and injects the resulting path-level structural evidence into each token in query and candidate entities to prompt LLMs. Experiments on JF17K, WikiPeople, and FB-AUTO demonstrate that HyperCoT consistently outperforms strong  $n$ -ary KGC baselines, particularly in high arity and structural sparsity scenarios, while yielding interpretable multi-hop reasoning traces.

## 1 Introduction

Knowledge hypergraphs, also known as  $n$ -ary knowledge graphs, represent facts governed by high-order interactions and role-dependent structural constraints. For instance, a manufacturing event may involve distinct entities, such as a vehicle model, brand, engine type, factory, and target mar-

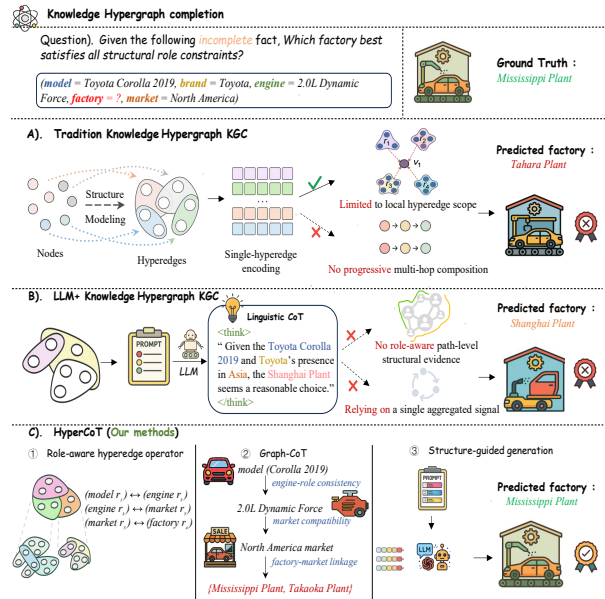


Figure 1: Motivating comparison of  $n$ -ary knowledge graph completion paradigms. Existing hypergraph models rely on single-hyperedge or final aggregated representations without progressive multi-hop evidence composition, while LLM-based approaches lack role-aware and path-level structural evidence.

ket, each playing a specific role. Such multi-arity facts are prevalent in various applications including question answering (Yani and Krisnadhi, 2021), recommendation (Chicaiza and Díaz, 2021), and decision support (Wang et al., 2023b). However, real-world knowledge hypergraphs are often incomplete, motivating the task of *knowledge hypergraph completion* (also called  $n$ -ary KGC), which aims to infer missing entities or relations within these multi-argument facts (Chen et al., 2020).

Early approaches extend embedding-based models for classical KGC tasks or adopt reification-based transformations to score each hyperedge as a whole (Wen et al., 2016; Zhang et al., 2020). More recent GNN-based hypergraph encoders establish interactions among the entities and their

roles with incidence structures (Zhou et al., 2023; Wang et al., 2023a; Li et al., 2025). Although architecturally different, these methods largely follow a *local hyperedge encoding* paradigm: scoring each hyperedge via learning aggregated representations from its constituent nodes and edges, without explicitly modeling step-by-step correlations between hyperedges to support progressive reasoning. Thus, they fail to effectively integrate the diverse high-order constraints embedded within hypergraphs. As shown in Figure 1(a), this paradigm can lead to incorrect yet locally plausible predictions (e.g., *Tahara Plant*).

In parallel, large language models (LLMs) have reformulated knowledge graph completion as a text generation task and achieved promising results, but just in classical binary or triple-based settings that lack hyperedge structures (Wei et al., 2024; Yang et al., 2025a). While LLMs exhibit a strong ability to associate multiple facts at the linguistic level through chain-of-thought (CoT) prompting in hypergraph QA tasks (Feng et al., 2024; Luo et al., 2025), they are typically guided by the isolated query hyperedge or a single aggregated signal, rather than explicit *path-level structural evidence* for multi-hop reasoning. This often results in predictions that are linguistically coherent but structurally inconsistent (e.g. *Shanghai Plant* in Figure 1(b)).

These observations highlight a core challenge in  $n$ -ary KGC: accurate prediction requires not only expressive node/edge representations, but also *explicit and role-aware reasoning rationales that preserve and compose structural evidence across multiple hops of hyperedges*. Neither enriched hyperedge embeddings nor language-driven generation alone can fulfil this requirement.

To address this challenge, we propose **HyperCoT**, a structure-aware approach for  $n$ -ary knowledge hypergraph completion. HyperCoT encodes hyperedges as propagatable structural states and performs attention-driven multi-hop reasoning to extract depth-sensitive and path-level structural evidence. By preserving and aggregating intermediate hyperedge states along reasoning paths, it constructs an explicit *Graphical Chain-of-Thought* (Graph-CoT), capturing both local (direct, near) and global (indirect, far) high-order correlations with varying degrees of contextual enhancement. This structured rationale is then injected into tokens of query and candidate entities to prompt LLMs for structure-guided prediction.

Our contributions are summarized as follows:

- We introduce **HyperCoT**, the first LLM-based structure-aware approach for  $n$ -ary knowledge hypergraph completion, which stimulate the potential of LLMs on role-aware multi-hop structural reasoning.
- We propose a Graphical Chain-of-Thought construction mechanism that preserves and aggregate intermediate structural evidence along reasoning paths, facilitating depth-sensitive feature enhancement.
- We develop a structure-guided generation operator that injects the resulting path-level evidence into individual tokens to prompt LLMs, thereby improving both accuracy and interpretability of link prediction in hypergraphs.

Experiments on JF17K, WikiPeople, and FB-AUTO show that HyperCoT consistently outperforms strong  $n$ -ary KGC baselines, especially in high arity and structural sparsity scenarios.

## 2 Related Work

We review related work on knowledge hypergraph completion and generation-based knowledge graph completion.

**Knowledge Hypergraph Completion.** Early knowledge graph completion methods focus on binary relations using embedding-based scoring functions, such as TransE (Bordes et al., 2013), DistMult (Yang et al., 2015), and RotatE (Sun et al., 2019). To extend these models to  $n$ -ary settings, prior work introduces reification, tuple representations, or role-aware projections, including m-TransH, NaLP, RAM, and ReAIE (Yang et al., 2015; Guan et al., 2019; Liu et al., 2021; Fatemi et al., 2023). More recent GNN-based methods model  $n$ -ary facts as hyperedges and perform message passing over incidence structures, such as HyperMLN, RD-MPNN, HyConvE, tNaLP+, and HyCubE (Chen et al., 2022; Zhou et al., 2023; Wang et al., 2023a; Guan et al., 2023; Li et al., 2025). Despite improved structural expressiveness, these approaches largely follow a *local hyperedge encoding* paradigm, scoring each hyperedge individually or based on a single aggregated representation, without preserving intermediate propagation states that encode depth-specific structural evidence across multiple hops.

**Generation-based KGC.** Another line of work formulates knowledge graph completion as a generation task, including sequence-to-sequence models such as KGT5 (Saxena et al., 2022), GenKGC (Xie et al., 2022), as well as recent LLM-based approaches leveraging instruction tuning or prompting with structural cues, e.g., DIFT (Liu et al., 2024), KICGPT (Wei et al., 2024), GS-KGC (Yang et al., 2025b), and SLiNT (Yang et al., 2025a). These methods demonstrate that LLMs are able to associate multiple facts during generation in classical binary or triple-based KGC. However, in  $n$ -ary or hypergraph settings with multiple interdependent facts, existing approaches often degenerate to exposing only isolated hyperedges or a single aggregated structural signal, as commonly observed in hypergraph QA tasks, rather than explicit path-level structural evidence capturing multi-hop, role-aware dependencies. In contrast, HyperCoT performs multi-hop structural reasoning over role-aware hyperedges, preserves intermediate propagation states, and injects the resulting path-level structural evidence into LLMs for structure-guided prediction.

### 3 Problem Formulation

#### 3.1 Knowledge Hypergraph

Given a finite set of entities  $\mathcal{V}$ , relations  $\mathcal{R}$ , and  $n$ -ary facts  $\mathcal{T}$ , a *knowledge hypergraph* is defined as  $\mathcal{H} = (\mathcal{V}, \mathcal{R}, \mathcal{T})$ . Each fact  $e \in \mathcal{T}$  is represented as an ordered tuple  $e = (r; u_1, u_2, \dots, u_n)$ , where  $r \in \mathcal{R}$  denotes an  $n$ -ary relation and  $u_i \in \mathcal{V}$  represents the entity participating in the  $i$ -th semantic role of relation  $r$ . We denote the entity at position  $i$  of hyperedge  $e$  by  $e(i) = u_i$ . A knowledge graph is a special case of a knowledge hypergraph with  $n = 2$ , i.e., all relations are binary.

#### 3.2 Knowledge Hypergraph Link Prediction

Let  $\mathcal{T}_O \subseteq \mathcal{T}$  denote the observed hyperedges. We consider  $n$ -ary knowledge hypergraph link prediction under the *single missing entity* setting. Given an incomplete query hyperedge  $e_q = (r; u_1, \dots, u_{i-1}, ?, u_{i+1}, \dots, u_n)$ , the task is to predict the missing entity  $u_i \in \mathcal{V}$  such that the completed hyperedge belongs to the unobserved set  $\mathcal{T} - \mathcal{T}_O$ . Following prior work, this task is formulated as ranking candidate entities from  $\mathcal{V}$  conditioned on the known context  $\tilde{u} = (u_1, \dots, u_{i-1}, u_{i+1}, \dots, u_n)$  and relation  $r$ .

## 4 Method

We propose **HyperCoT**, a structure-aware approach for knowledge hypergraph link prediction built upon LLMs. HyperCoT models a query hyperedge as a propagatable high-order structural state, performs multi-hop reasoning over the hypergraph, and aggregates structural evidence into a *Graphical Chain-of-Thought (Graph-CoT)* for structure-guided prediction. An overview of the approach is shown in Figure 2.

### 4.1 High-Order Structural State Learning

For an  $n$ -ary hyperedge, semantics arise from interactions among entities playing different roles under a given relation. To preserve such role-dependent interactions, HyperCoT constructs a *high-order structural state* by projecting each entity instance into a relation- and role-aware subspace:

$$h_{e,u_i} = W_{r(e),i} \hat{h}_{e,u_i}, \quad (1)$$

where  $\hat{h}_{e,u_i}$  denotes the raw feature of entity  $u_i$  when it appears at the  $i$ -th role of hyperedge  $e$ , and  $W_{r(e),i} \in \mathbb{R}^{d \times d}$  is a learnable projection matrix specific to the relation  $r(e)$  and the role index  $i$ . In practice, each  $W_{r(e),i}$  is parameterized in a low-rank form  $W_{r(e),i} = A_{r(e)} B_i^\top$ , where  $A_{r(e)}, B_i \in \mathbb{R}^{d \times d_r}$  and  $d_r \ll d$ .

To capture explicit interactions among different roles under a given relation, we define a learnable role-pair interaction operator that jointly encodes the corresponding role-aware entity embeddings and the relation embedding:

$$\psi(\mathcal{X}_e(i, j)) = \sigma(W_\psi [h_{e,u_i} \parallel h_{e,u_j} \parallel h_r]), \quad (2)$$

where  $\parallel$  denotes concatenation,  $h_r$  is the embedding of relation  $r$ ,  $W_\psi \in \mathbb{R}^{d' \times 3d}$  is a learnable parameter matrix, and  $\sigma(\cdot)$  is instantiated as the ReLU activation function (Nair and Hinton, 2010). The resulting representation  $\psi(\mathcal{X}_e(i, j))$  captures second-order and relation-conditioned interactions between roles  $(i, j)$ , which serves as a compact structural feature for subsequent aggregation.

Then, all role-pair interaction features are aggregated using structural attention:

$$\alpha_{ij} = \text{softmax}_{i,j} \left( u^\top \psi(\mathcal{X}_e(i, j)) \right), \quad (3)$$

where  $u \in \mathbb{R}^{d'}$  is a learnable attention vector. The initial hyperedge structural state is computed as

$$h_e^{(0)} = W_s \sum_{i,j} \alpha_{ij} \psi(\mathcal{X}_e(i, j)), \quad (4)$$

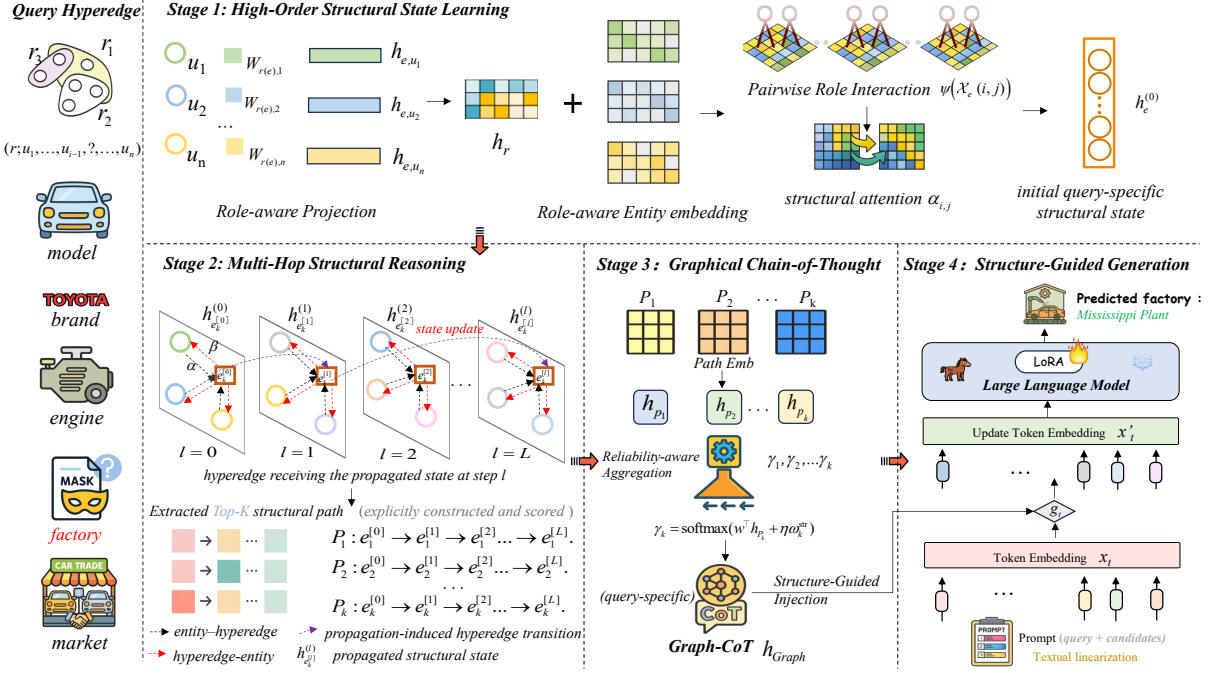


Figure 2: **Overview of HyperCoT.** Given an  $n$ -ary query hyperedge  $e_q = (r; u_1, \dots, u_{i-1}, ?, u_{i+1}, \dots, u_n)$ , HyperCoT learns an initial structural state, performs multi-hop propagation to extract top- $K$  structural paths, and aggregates them into a Graph-CoT for structure-guided prediction.

where  $W_s \in \mathbb{R}^{d \times d'}$  maps interaction features to the structural state space.

## 4.2 Multi-Hop Structural Reasoning

HyperCoT performs multi-hop structural reasoning by iteratively propagating a query-conditioned structural state over the incidence structure of the knowledge hypergraph. Entities are initialized with embeddings  $h_v^{(0)}$ , and the query hyperedge starts from a structural state  $h_{e_q}^{(0)}$  (Eq. 4), which are mutually updated in a shared space.

Let  $h_v^{(l)}$  and  $h_e^{(l)}$  denote the structural states of entity  $v$  and hyperedge  $e$  after the  $l$ -th aggregation step, respectively. We denote by  $\mathcal{N}_E(v) = \{e \mid v \in e\}$  the set of hyperedges incident to entity  $v$ . At each step, bidirectional propagation is performed as:

$$\begin{aligned} h_e^{(l+1)} &= \sum_{v \in e} \alpha_{v,e}^{(l)} h_v^{(l)}, \\ h_v^{(l+1)} &= \sum_{e \in \mathcal{N}_E(v)} \beta_{e,v}^{(l)} h_e^{(l)}, \end{aligned} \quad (5)$$

where  $\alpha_{v,e}^{(l)}$  and  $\beta_{e,v}^{(l)}$  are normalized attention weights computed via dot-product between entity and hyperedge states, followed by softmax normalization over the corresponding neighborhoods.

**Structural path extraction.** HyperCoT performs attention-driven multi-hop reasoning over propagatable hyperedge states, explicitly preserving intermediate states to extract *depth-sensitive* structural paths. Early hops near the query emphasize local role compatibility, while later hops encode global and indirect structural constraints. Here,  $L$  denotes the depth of multi-hop reasoning, i.e., the number of propagation steps used to extract  $L$ -hop structural paths. Let  $\mathcal{N}_H(e)$  denote the set of hyperedges that share at least one entity with hyperedge  $e$ . The set of candidate  $L$ -hop paths can be defined as:

$$\tilde{\mathcal{P}}_L = \{\langle e^{[0]}, \dots, e^{[L]} \rangle \mid e^{[0]} = e_q, e^{[l+1]} \in \mathcal{N}_H(e^{[l]})\}. \quad (6)$$

Notice that the complicated correlations within the query hyperedge are mainly reflected in original features, while indirect correlations can be captured by far hyperedges in the path through enriched representations. Therefore, we devise a synchronized unrolling of propagation and path expansion, such that the  $l$ -th hyperedge along the path  $P_k$  corresponds to its structural state  $h_{e_k}^{(l)}$  after the  $l$ -th propagation step. On this basis, for two consecutive hyperedges  $e^{[l]}$  and  $e^{[l+1]} \in \mathcal{N}_H(e^{[l]})$  along a candidate path, we define a propagation-induced

transition score in the corresponding step as:

$$\pi^{[l]}(e^{[l]} \rightarrow e^{[l+1]}) = \sum_{v \in e^{[l]} \cap e^{[l+1]}} \alpha_{v, e^{[l]}}^{(l)} \beta_{e^{[l+1]}, v}^{(l)}. \quad (7)$$

Each candidate structural path  $\langle e^{[0]}, \dots, e^{[l]} \rangle$  is then scored by its cumulative transition strength:

$$\text{Score}(\langle e^{[0]}, \dots, e^{[l]} \rangle) = \sum_{l=0}^{L-1} \log \pi^{[l]}(e^{[l]} \rightarrow e^{[l+1]}). \quad (8)$$

Since  $|\tilde{\mathcal{P}}_L|$  grows exponentially with  $L$ , we apply beam-style pruning based on the path scores above to retain the top- $K$  structural paths  $\{P_k\}_{k=1}^K$ . The complete procedure is provided in Appendix B.

**Depth-sensitive path embedding.** Each path is embedded via depth-aware aggregation:

$$h_{P_k} = \sum_{l=1}^L \omega_l^{[k]} h_{e_k^{[l]}}^{(l)}, \quad (9)$$

where the hop-specific weights are calculated by

$$\omega_l^{[k]} = \frac{\pi^{[l-1]}(e_k^{[l-1]} \rightarrow e_k^{[l]})}{\sum_{j=1}^L \pi^{[j-1]}(e_k^{[j-1]} \rightarrow e_k^{[j]})}. \quad (10)$$

### 4.3 Graphical Chain-of-Thought Construction

Given the extracted structural path embeddings  $\{h_{P_k}\}_{k=1}^K$ , HyperCoT aggregates them into a single query-specific structural representation, termed *Graphical Chain-of-Thought (Graph-CoT)*.

Formally, the Graph-CoT for a query hyperedge  $e_q$  is constructed as

$$h_{\text{Graph}}(e_q) = \sum_{k=1}^K \gamma_k g(h_{P_k}), \quad (11)$$

where  $g(\cdot)$  is a ReLU-based projection function that maps path embeddings into the shared structural representation space. The aggregation weight  $\gamma_k$  reflects the relative contribution of each structural path and is computed by combining semantic compatibility and structure-aware reliability:

$$\gamma_k = \text{softmax}_k(w^\top h_{P_k} + \eta \pi_k^{\text{str}}), \quad (12)$$

where  $w$  is a learnable scoring vector,  $\eta$  is a scalar hyperparameter, and  $\pi_k^{\text{str}}$  is a path-level structural reliability score that summarizes the propagation-induced transition score  $\pi^{[l]}$  along path  $P_k$ , reflecting how reliably structural constraints are preserved across multiple hops. Theoretical justification of Graph-CoT aggregation is provided in Appendix A.

### 4.4 Structure-Guided Generation

HyperCoT incorporates the constructed Graph-CoT into prediction via a structure-guided generation operator, where structural reasoning is performed entirely in the hypergraph space and injected to guide language-based scoring.

Given a query hyperedge  $e_q$ , we linearize it into a structured natural language prompt using a fixed template (see Appendix E), which specifies the incomplete  $n$ -ary fact and a constrained candidate entity set. Let  $x_t$  denote the embedding of the  $t$ -th token in the structured prompt that contains the query hyperedge and candidate entity representations. Graph-CoT is injected at the embedding level through a gating mechanism:

$$\begin{aligned} x'_t &= g_t \odot h_{\text{Graph}}(e_q) + (1 - g_t) \odot x_t, \\ g_t &= \sigma(W_g (h_{\text{Graph}}(e_q) \parallel x_t)), \end{aligned} \quad (13)$$

where  $g_t \in \mathbb{R}^d$  is a learned gating vector based on the original token and graph evidence,  $W_g \in \mathbb{R}^{d \times 2d}$  is a learnable projection matrix, and  $\odot$  denotes element-wise multiplication.

Then, the structure-modulated embeddings  $\{x'_t\}_{t=1}^T$  are fed into an LLM to obtain a token-level conditional distribution:

$$p(\cdot | e_q, h_{\text{Graph}}(e_q)) = \text{LLM}(\{x'_t\}_{t=1}^T). \quad (14)$$

For scalability, the prediction is performed under a candidate-constrained setting. An embedding-based  $n$ -ary link prediction model NaLP (Guan et al., 2019) is employed to retrieve the top-20 candidates, yielding the candidate set  $\mathcal{C}(e_q)$ . The language model scores only this reduced set in a discriminative manner.

Each candidate entity  $v \in \mathcal{C}(e_q)$  is scored by the conditional log-likelihood of its tokenized name:

$$s(v) = \sum_{m=1}^{|v|} \log p(t_m^v | e_q, h_{\text{Graph}}(e_q), t_{< m}^v), \quad (15)$$

where  $\{t_m^v\}_{m=1}^{|v|}$  denotes the token sequence of entity  $v$ . The final prediction result is

$$\hat{v} = \arg \max_{v \in \mathcal{C}(e_q)} s(v). \quad (16)$$

### 4.5 Training Objective

HyperCoT is trained by jointly optimizing entity prediction accuracy and structural alignment:

$$\mathcal{L} = \mathcal{L}_{\text{pred}} + \lambda \mathcal{L}_{\text{align}}, \quad (17)$$

where  $\mathcal{L}_{\text{pred}}$  is the negative log-likelihood of the ground-truth entity under the candidate-constrained scoring distribution (Eq. 15), and  $\mathcal{L}_{\text{align}}$  regularizes the consistency between the constructed Graph-CoT representation and the correct entity in the structural embedding space. The scalar  $\lambda$  controls the strength of structural regularization. Details of  $\mathcal{L}_{\text{align}}$  are provided in Appendix F.

## 5 Experiments

Our experiments are designed to answer the following four research questions: (RQ1) Does HyperCoT outperform state-of-the-art  $n$ -ary KGC methods across diverse benchmarks? (RQ2) Are the performance gains mainly attributable to explicit multi-hop structural reasoning rather than stronger encoders or larger model capacity? (RQ3) How robust is HyperCoT under challenging structural conditions, such as structural sparsity and incompleteness? (RQ4) How sensitive is HyperCoT to its hyperparameter settings?

### 5.1 Experimental Setup

**Datasets.** We evaluate on three  $n$ -ary knowledge hypergraph benchmarks: JF17K (Liu et al., 2021), FB-AUTO (Fatemi et al., 2020), and WikiPeople (Guan et al., 2019), which vary in arity, sparsity, and structural complexity. Detailed statistics are provided in Appendix D.

**Baselines.** We compare HyperCoT with representative  $n$ -ary KGC methods from three categories: (1) **Embedding-based models**, including RAE (Zhang et al., 2018) and NaLP (Guan et al., 2019); (2) **Semantic matching models**, including HypE (Fatemi et al., 2020), RAM (Liu et al., 2021), PosKHG (Chen et al., 2023), and ReAIE (Fatemi et al., 2023); as well as (3) **GNN-based models**, including HyperMLN (Chen et al., 2022), tNaLP+ (Guan et al., 2023), RD-MPNN (Zhou et al., 2023), HyConvE (Wang et al., 2023a), and the cubical structural encoders HyCubE/HyCubE+ (Li et al., 2025). In addition, we compare HyperCoT with several LLM baselines under both fine-tuned and zero-shot settings, focusing on models with comparable capacity (e.g., 7B–10B). Detailed configurations are provided in Appendix D.2.

**Evaluation Metrics.** Following standard practice, we report Mean Reciprocal Rank (MRR) and Hits@K ( $K = 1, 3, 10$ ) under the filtered evaluation protocol.

**Training Setup.** HyperCoT is trained on LLaMA-3-8B-Instruct using a parameter-efficient fine-tuning strategy. Detailed implementation and hyperparameter settings are provided in Appendix D.

### 5.2 Main Results (RQ1)

Table 1 summarizes the performance of HyperCoT on three representative benchmarks.

**Overall performance across datasets.** Overall, HyperCoT achieves consistently strong results across all datasets, demonstrating robust generalization under various structural settings. On JF17K, which exhibits complex relational structures and diverse role configurations, HyperCoT achieves the best overall performance, improving MRR from 0.584 (HyCubE) to 0.599 and consistently outperforming all baselines across evaluation metrics. On the more sparse and noisy WikiPeople dataset, HyperCoT attains the highest MRR (0.451) and competitive Hits@1/10, indicating improved robustness under incomplete and noisy structural contexts. On FB-AUTO, which features strong type constraints and well-structured relations, HyperCoT achieves the best overall ranking performance, improving Hits@10 by +0.012 over HyCubE+. We further analyze the computational efficiency and overhead of HyperCoT in Appendix C.

**Comparison with structural and semantic baselines.** HyperCoT consistently outperforms embedding-based and semantic matching models, which rely on local or role-level scoring without explicit multi-hop composition. For example, HyperCoT surpasses HyperMLN by +0.043 MRR on JF17K and +0.100 on WikiPeople, validating the benefit of preserving intermediate structural states in the reasoning process.

**Comparison with GNN-based models.** GNN-based models propagate information via message passing but typically compress structural cues from different depths into a single representation, obscuring the distinction between early-hop role compatibility and later-hop global correlations. By explicitly constructing and aggregating multi-hop reasoning paths, HyperCoT consistently outperforms these models, e.g., by +0.087 MRR over RD-MPNN and +0.019 over HyConvE on JF17K, and +0.057 over HyConvE on FB-AUTO.

**Comparison with comparable-scale language models.** We evaluate several language models

Table 1: Results of link prediction on  $n$ -arity knowledge hypergraph datasets. Best results are shown in **bold**, and second-best ones are underlined. Results not reported in the original papers and obtained locally are marked with †.

Model	JF17K				WikiPeople				FB-AUTO			
	MRR	Hits@1	Hits@3	Hits@10	MRR	Hits@1	Hits@3	Hits@10	MRR	Hits@1	Hits@3	Hits@10
RAE	0.392	0.312	0.433	0.561	0.253	0.118	0.343	0.463	0.703	0.614	0.764	0.854
NaLP	0.310	0.239	0.334	0.450	0.338	0.272	0.362	0.466	0.672	0.611	0.712	0.774
HypE	0.494	0.399	0.532	0.650	0.263	0.127	0.355	0.486	0.804	0.774	0.824	0.856
RAM	0.539	0.463	0.573	0.690	0.363	0.271	0.405	0.500	0.830	0.803	0.851	0.876
PosKHG	0.545	0.469	0.582	0.706	0.315†	0.214†	0.377†	0.475†	0.856	0.821	0.876	0.895
ReAIE	0.530	0.454	0.563	0.677	0.332†	0.207†	0.417†	0.514†	0.861	0.836	0.877	0.908
HyperMLN	0.556	0.482	0.597	0.717	0.351†	0.270†	0.394†	0.497†	0.831	0.803	0.851	0.877
tNaLP+	0.449	0.370	0.484	0.598	0.339	0.269	0.369	0.473	0.729	0.645	0.748	0.826
RD-MPNN	0.512	0.445	0.573	0.685	–	–	–	–	0.810	0.714	0.880	0.888
HyConvE	0.580	0.478	0.610	0.729	0.362	0.275	0.388	0.501	0.847	0.820	0.872	0.901
HyCubE	<u>0.584</u>	<u>0.508</u>	<u>0.616</u>	<u>0.730</u>	<u>0.448</u>	<b>0.368</b>	<u>0.490</u>	<u>0.592</u>	<u>0.881</u>	<u>0.860</u>	<u>0.894</u>	<u>0.918</u>
HyCubE+	0.582	<u>0.511</u>	0.611	0.720	0.433	0.347	0.478	0.591	<u>0.891</u>	<u>0.872</u>	<u>0.901</u>	<u>0.923</u>
<b>HyperCoT (Ours)</b>	<b>0.599</b>	<b>0.527</b>	<b>0.634</b>	<b>0.743</b>	<b>0.451</b>	<u>0.366</u>	<b>0.495</b>	<b>0.612</b>	<b>0.904</b>	<b>0.883</b>	<b>0.912</b>	<b>0.927</b>

Table 2: Comparison with same-scale LLMs on JF17K.

Model (7B–10B)	MRR	Hits@1	Hits@10
LLaMA-2-7B (FT)	0.489	0.401	0.655
Mistral-7B-Instruct (FT)	0.512	0.419	0.671
Qwen-2-7B-Chat (FT)	0.524	0.436	0.682
Gemma-2-9B-Instruct (FT)	0.538	0.447	0.695
GPT-4o-mini (Zero-shot)	0.521	0.432	0.681
<b>LLaMA-3-8B-Instruct (FT)</b>	0.551	0.463	0.708
<b>HyperCoT (Ours)</b>	<b>0.599</b>	<b>0.527</b>	<b>0.743</b>

with comparable capacity (7B–10B parameters) under consistent fine-tuning or zero-shot protocols to form fair and reasonable baselines. As shown in Table 2, LLaMA-3-8B-Instruct performs best among these models and is thus adopted as the backbone for HyperCoT. Under the same setting, HyperCoT yields +0.044 MRR improvement on JF17K, demonstrating the benefit of injecting explicit structural evidence.

### 5.3 Ablation Study (RQ2)

To assess the contribution of each component in HyperCoT, we conduct ablation studies by removing one module at a time while keeping all others fixed. The evaluated variants include: (1) **w/o High-order Structural State Learning**, removing role-aware structural encoding; (2) **w/o Progressive Multi-hop Reasoning**, disabling iterative structural propagation and utilizing only the initial query state; (3) **w/o Intermediate State Aggregation**, retaining multi-hop propagation but using only the final structural state; (4) **w/o Path-level Adaptive Aggregation**, replacing path-level weighting with uniform averaging; (5) **w/o Structural Alignment**, removing the structural–semantic alignment loss; and (6) **w/o Structural Injection**, disabling structure-guided information in prompts.

**Ablation Analysis.** Table 3 reports the ablation results of HyperCoT across three benchmarks. Removing any major component consistently degrades performance, confirming that all modules contribute to the overall effectiveness. Disabling *progressive multi-hop reasoning* and using only the initial query state leads to the largest performance drop across datasets, showing that local hyperedge representations alone are insufficient for  $n$ -ary knowledge graph completion. Even when multi-hop propagation is retained, removing *intermediate state aggregation* and relying solely on the final structural state still reduces the prediction accuracy, indicating that intermediate hyperedge states encode complementary structural evidence beyond a single final signal, and they should be utilized according to the path depth to realize varying degrees of feature enhancement.

The impact of other components is dataset-dependent: on JF17K and WikiPeople, high-order structural state learning and path-level aggregation are more critical, while on FB-AUTO our approach is more sensitive to structure-guided injection.

### 5.4 Structural Robustness Analysis (RQ3)

We evaluate the robustness of HyperCoT under structural sparsity and graph incompleteness.

(1) **Degree Sparsity.** We group entities by degree and evaluate performance on the bottom 20%. As shown in Table 4, HyperCoT consistently outperforms strong baselines in this long-tail regime, demonstrating stronger generalization under sparse structural context.

(2) **Random Edge Drop.** We randomly remove 10–40% of hyperedges to simulate incomplete hypergraphs. Figure 3 shows the resulting MRR

Table 3: Ablation results across three benchmarks. Best results are shown in **bold**, and second-best underlined.

Variant	JF17K				WikiPeople				FB-AUTO			
	MRR	H@1	H@3	H@10	MRR	H@1	H@3	H@10	MRR	H@1	H@3	H@10
w/o High-order Structural State Learning	0.574	0.501	0.616	0.733	0.432	0.346	0.474	0.595	0.889	0.868	0.900	0.926
w/o Progressive Multi-hop Reasoning	0.564	0.487	0.602	0.720	0.421	0.331	0.460	0.574	0.882	0.861	0.896	0.919
w/o Intermediate State Aggregation	0.581	0.513	0.621	0.731	0.436	0.349	0.480	0.600	0.893	0.871	0.904	0.924
w/o Path-level Adaptive Aggregation	0.579	0.504	0.618	0.734	0.437	0.351	0.482	0.603	0.896	0.874	0.906	0.923
w/o Structural Alignment	0.583	0.511	0.623	<u>0.741</u>	0.438	0.353	0.484	0.604	0.894	0.872	0.904	0.922
w/o Structural Injection	<u>0.587</u>	<u>0.514</u>	<u>0.627</u>	0.740	<u>0.441</u>	<u>0.357</u>	<u>0.488</u>	<u>0.607</u>	0.891	0.870	0.902	0.923
<b>Full HyperCoT</b>	<b>0.599</b>	<b>0.527</b>	<b>0.634</b>	<b>0.743</b>	<b>0.451</b>	<b>0.366</b>	<b>0.495</b>	<b>0.612</b>	<b>0.904</b>	<b>0.883</b>	<b>0.912</b>	<b>0.927</b>

Table 4: MRR on low-degree entities (bottom 20%). HyperCoT outperforms the baseline HyCubE+ by +0.024 on average.

Model	JF17K	WikiPeople	FB-AUTO
HyConvE	0.421	0.298	0.762
HyCubE+	0.458	0.331	0.787
<b>HyperCoT</b>	<b>0.482</b>	<b>0.354</b>	<b>0.801</b>

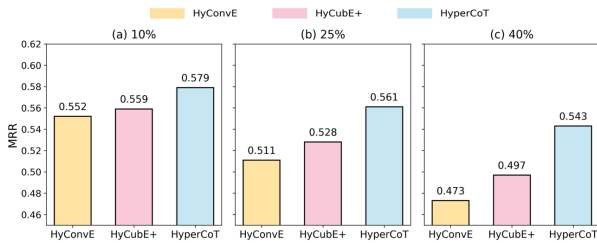


Figure 3: MRR degradation under random hyperedge deletion on JF17K.

degradation on JF17K, demonstrating improved robustness to structural incompleteness. Qualitative case studies are provided in Appendix G.

### 5.5 Hyperparameter Sensitivity Analysis (RQ4)

We analyze the sensitivity of HyperCoT on key hyperparameters that control its structural reasoning behaviors.

**Effect of reasoning depth  $L$ .** We vary the reasoning depth  $L \in \{1, 2, 3, 4\}$ . As shown in Fig. 4(a), performance improves from  $L = 1$  to  $L = 3$  across all datasets, reflecting the benefit of progressive multi-hop structural reasoning. Further increasing the depth to  $L = 4$  yields marginal or degraded performance, indicating diminishing returns from overly deep reasoning. Accordingly, we set  $L = 3$  as the default depth.

**Effect of structural path number  $K$ .** We further examine the impact of the number of extracted Graph-CoT paths  $K \in \{1, 3, 5, 7\}$ . As shown in Fig. 4(b), performance improves consistently as  $K$  increases up to 5, confirming the benefit of ag-

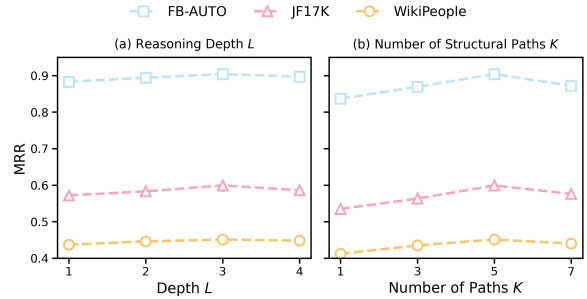


Figure 4: Sensitivity analysis of key hyperparameters. (a) Effect of reasoning depth  $L$ . (b) Effect of structural path number  $K$ .

gregating multiple high-quality reasoning paths. When  $K$  is further increased to 7, performance saturates or slightly degrades, indicating diminishing returns from redundant paths. Accordingly, we adopt  $K = 5$  in all experiments.

Sensitivity analyses of additional hyperparameters, including the structural alignment weight  $\lambda$  and the path reliability coefficient  $\eta$ , are reported in Appendix D.3.

## 6 Conclusion

We presented **HyperCoT**, a structure-aware LLM-based approach for  $n$ -ary knowledge graph completion that integrates multi-hop structural reasoning with structure-guided generation. By modeling and aggregating *intermediate hyperedge states* along reasoning paths, HyperCoT constructs a Graphical Chain-of-Thought that captures depth-sensitive structural evidence beyond a single final representation, and effectively stimulates the potential of LLMs in the underexplored field, knowledge hypergraph link prediction. Experiments across multiple benchmarks show that HyperCoT consistently improves performance under high-arity and structurally sparse settings, highlighting the importance of progressive structural evidence accumulation for reliable  $n$ -ary knowledge graph completion.

## 583 Limitations

584 HyperCoT is designed to operate on structured  
585 knowledge hypergraphs and focuses on reasoning  
586 over relational structures. While this work does not  
587 explicitly incorporate multimodal signals, extend-  
588 ing the approach to support multimodal or weakly  
589 structured inputs is a natural direction for future  
590 research. Moreover, integrating HyperCoT with au-  
591 tomatic structure construction or noisy real-world  
592 knowledge sources may further broaden its appli-  
593 cability.

## 594 Ethical Considerations

595 All datasets used are public and contain no sensitive  
596 information. No human subjects are involved.

## 597 References

598 Antoine Bordes, Nicolas Usunier, Alberto García-  
599 Durán, Jason Weston, and Oksana Yakhnenko.  
600 2013. [Translating embeddings for modeling multi-  
601 relational data](#). In *Advances in Neural Information  
602 Processing Systems 26: 27th Annual Conference on  
603 Neural Information Processing Systems 2013. Pro-  
604 ceedings of a meeting held December 5-8, 2013, Lake  
605 Tahoe, Nevada, United States*, pages 2787–2795.

606 Zhe Chen, Yuehan Wang, Bin Zhao, Jing Cheng, Xin  
607 Zhao, and Zongtao Duan. 2020. [Knowledge graph  
608 completion: A review](#). *IEEE Access*, 8:192435–  
609 192456.

610 Zirui Chen, Xin Wang, Chenxu Wang, and Jianxin Li.  
611 2022. [Explainable link prediction in knowledge hy-  
612 pergraphs](#). In *Proceedings of the 31st ACM Interna-  
613 tional Conference on Information & Knowledge Man-  
614 agement, Atlanta, GA, USA, October 17-21, 2022*,  
615 pages 262–271. ACM.

616 Zirui Chen, Xin Wang, Chenxu Wang, and Zhao Li.  
617 2023. [Poskkg: A position-aware knowledge hyper-  
618 graph model for link prediction](#). *Data Sci. Eng.*,  
619 8(2):135–145.

620 Janneth Chicaiza and Priscila Valdiviezo Díaz. 2021.  
621 [A comprehensive survey of knowledge graph-based  
622 recommender systems: Technologies, development,  
623 and contributions](#). *Inf.*, 12(6):232.

624 Bahare Fatemi, Perouz Taslakian, David Vázquez, and  
625 David Poole. 2020. [Knowledge hypergraphs: Pre-  
626 diction beyond binary relations](#). In *Proceedings of  
627 the Twenty-Ninth International Joint Conference on  
628 Artificial Intelligence, IJCAI 2020*, pages 2191–2197.  
629 ijcai.org.

630 Bahare Fatemi, Perouz Taslakian, David Vázquez, and  
631 David Poole. 2023. [Knowledge hypergraph embed-  
632 ding meets relational algebra](#). *J. Mach. Learn. Res.*,  
633 24:105:1–105:34.

Yifan Feng, Chengwu Yang, Xingliang Hou, Shaoyi  
634 Du, Shihui Ying, Zongze Wu, and Yue Gao. 2024.  
635 [Beyond graphs: Can large language models compre-  
636 hend hypergraphs?](#) *Preprint*, arXiv:2410.10083.  
637

Google DeepMind. 2024. [Gemma 2 technical report](#).  
638 Technical report, Google DeepMind.  
639

Aaron Grattafiori, Abhimanyu Dubey, Abhinav Jauhri,  
640 Abhinav Pandey, Abhishek Kadian, Ahmad Al-  
641 Dahle, Aiesha Letman, Akhil Mathur, Alan Schel-  
642 ten, Alex Vaughan, Amy Yang, Angela Fan, Anirudh  
643 Goyal, Anthony Hartshorn, Aobo Yang, Archi Mi-  
644 tra, Archie Sravankumar, Artem Korenev, Arthur  
645 Hinsvark, and 542 others. 2024. [The llama 3 herd of  
646 models](#). *Preprint*, arXiv:2407.21783.  
647

Saiping Guan, Xiaolong Jin, Jiafeng Guo, Yuanzhuo  
648 Wang, and Xueqi Cheng. 2023. [Link prediction on  
649 n-ary relational data based on relatedness evaluation](#).  
650 *IEEE Trans. Knowl. Data Eng.*, 35(1):672–685.  
651

Saiping Guan, Xiaolong Jin, Yuanzhuo Wang, and  
652 Xueqi Cheng. 2019. [Link prediction on n-ary re-  
653 lational data](#). In *The World Wide Web Conference,  
654 WWW '19*, page 583–593, New York, NY, USA.  
655 Association for Computing Machinery.  
656

Edward J. Hu, Yelong Shen, Phillip Wallis, Zeyuan  
657 Allen-Zhu, Yuanzhi Li, Shean Wang, Lu Wang, and  
658 Weizhu Chen. 2022. [Lora: Low-rank adaptation of  
659 large language models](#). In *The Tenth International  
660 Conference on Learning Representations, ICLR 2022,  
661 Virtual Event, April 25-29, 2022*. OpenReview.net.  
662

Albert Q. Jiang, Alexandre Sablayrolles, Arthur Men-  
663 sch, Chris Bamford, Devendra Singh Chaplot, Diego  
664 de las Casas, Florian Bressand, Gianna Lengyel, Guil-  
665 laume Lample, Lucile Saulnier, Léo Renard Lavaud,  
666 Marie-Anne Lachaux, Pierre Stock, Teven Le Scao,  
667 Thibaut Lavril, Thomas Wang, Timothée Lacroix,  
668 and William El Sayed. 2023. [Mistral 7b](#). *Preprint*,  
669 arXiv:2310.06825.  
670

Zhao Li, Xin Wang, Jun Zhao, Wenbin Guo, and Jianxin  
671 Li. 2025. [Hycube: Efficient knowledge hypergraph  
672 3d circular convolutional embedding](#). *IEEE Trans.  
673 Knowl. Data Eng.*, 37(4):1902–1914.  
674

Yang Liu, Xiaobin Tian, Zequn Sun, and Wei Hu. 2024.  
675 [Finetuning generative large language models with  
676 discrimination instructions for knowledge graph com-  
677 pletion](#). In *The Semantic Web - ISWC 2024 - 23rd  
678 International Semantic Web Conference, Baltimore,  
679 MD, USA, November 11-15, 2024, Proceedings, Part  
680 I*, volume 15231 of *Lecture Notes in Computer Sci-  
681 ence*, pages 199–217. Springer.  
682

Yu Liu, Quanming Yao, and Yong Li. 2021. [Role-aware  
683 modeling for n-ary relational knowledge bases](#). In  
684 *Proceedings of the Web Conference 2021, WWW '21*,  
685 page 2660–2671, New York, NY, USA. Association  
686 for Computing Machinery.  
687

Haoran Luo, Haihong E, Guanting Chen, Yandan Zheng,  
688 Xiaobao Wu, Yikai Guo, Qika Lin, Yu Feng, Ze-min  
689

690	Kuang, Meina Song, Yifan Zhu, and Luu Anh Tuan. 2025. <a href="#">Hypergraphrag: Retrieval-augmented generation with hypergraph-structured knowledge representation</a> . <i>CoRR</i> , abs/2503.21322.	
691		
692		
693		
694	Vinod Nair and Geoffrey E. Hinton. 2010. <a href="#">Rectified linear units improve restricted boltzmann machines</a> . In <i>Proceedings of the 27th International Conference on Machine Learning (ICML-10), June 21-24, 2010, Haifa, Israel</i> , pages 807–814. Omnipress.	
695		
696		
697		
698		
699	OpenAI. 2024. <a href="#">GPT-4o mini: Advancing cost-efficient intelligence</a> .	
700		
701	Apoorv Saxena, Adrian Kochsiek, and Rainer Gemulla. 2022. <a href="#">Sequence-to-sequence knowledge graph completion and question answering</a> . In <i>Proceedings of the 60th Annual Meeting of the Association for Computational Linguistics (Volume 1: Long Papers), ACL 2022, Dublin, Ireland, May 22-27, 2022</i> , pages 2814–2828. Association for Computational Linguistics.	
702		
703		
704		
705		
706		
707		
708	Zhiqing Sun, Zhi-Hong Deng, Jian-Yun Nie, and Jian Tang. 2019. <a href="#">Rotate: Knowledge graph embedding by relational rotation in complex space</a> . In <i>7th International Conference on Learning Representations, ICLR 2019, New Orleans, LA, USA, May 6-9, 2019</i> . OpenReview.net.	
709		
710		
711		
712		
713		
714	Hugo Touvron, Louis Martin, Kevin Stone, Peter Albert, Amjad Almahairi, Yasmine Babaei, Nikolay Bashlykov, Soumya Batra, Prajwal Bhargava, Shruti Bhosale, Dan Bikel, Lukas Blecher, Cristian Canton-Ferrer, Moya Chen, Guillem Cucurull, David Esiobu, Jude Fernandes, Jeremy Fu, Wenyin Fu, and 49 others. 2023. <a href="#">Llama 2: Open foundation and fine-tuned chat models</a> . <i>CoRR</i> , abs/2307.09288.	
715		
716		
717		
718		
719		
720		
721		
722	Chenxu Wang, Xin Wang, Zhao Li, Zirui Chen, and Jianxin Li. 2023a. <a href="#">Hyconve: A novel embedding model for knowledge hypergraph link prediction with convolutional neural networks</a> . In <i>Proceedings of the ACM Web Conference 2023, WWW 2023, Austin, TX, USA, 30 April 2023 - 4 May 2023</i> , pages 188–198. ACM.	
723		
724		
725		
726		
727		
728		
729	Yu Wang, Feng Ye, Binqian Li, Gaoyang Jin, Dong Xu, and Fengsheng Li. 2023b. <a href="#">Urbanfloodkg: An urban flood knowledge graph system for risk assessment</a> . In <i>Proceedings of the 32nd ACM International Conference on Information and Knowledge Management, CIKM '23</i> , page 2574–2584, New York, NY, USA. Association for Computing Machinery.	
730		
731		
732		
733		
734		
735		
736	Yanbin Wei, Qiushi Huang, James T. Kwok, and Yu Zhang. 2024. <a href="#">KICGPT: large language model with knowledge in context for knowledge graph completion</a> . <i>CoRR</i> , abs/2402.02389.	
737		
738		
739		
740	Jianfeng Wen, Jianxin Li, Yongyi Mao, Shini Chen, and Richong Zhang. 2016. On the representation and embedding of knowledge bases beyond binary relations. In <i>Proceedings of the Twenty-Fifth International Joint Conference on Artificial Intelligence, IJCAI'16</i> , page 1300–1307. AAAI Press.	
741		
742		
743		
744		
745		
	Xin Xie, Ningyu Zhang, Zhoubo Li, Shumin Deng, Hui Chen, Feiyu Xiong, Mosha Chen, and Huajun Chen. 2022. <a href="#">From discrimination to generation: Knowledge graph completion with generative transformer</a> . In <i>Companion of The Web Conference 2022, Virtual Event / Lyon, France, April 25 - 29, 2022</i> , pages 162–165. ACM.	746
		747
		748
		749
		750
		751
		752
	An Yang, Baosong Yang, Binyuan Hui, Bo Zheng, Bowen Yu, Chang Zhou, Chengpeng Li, Chengyuan Li, Dayiheng Liu, Fei Huang, Guanting Dong, Huaran Wei, Huan Lin, Jialong Tang, Jialin Wang, Jian Yang, Jianhong Tu, Jianwei Zhang, Jianxin Ma, and 43 others. 2024. <a href="#">Qwen2 technical report</a> . <i>Preprint</i> , arXiv:2407.10671.	753
		754
		755
		756
		757
		758
		759
	Bishan Yang, Wen-tau Yih, Xiaodong He, Jianfeng Gao, and Li Deng. 2015. <a href="#">Embedding entities and relations for learning and inference in knowledge bases</a> . In <i>3rd International Conference on Learning Representations, ICLR 2015, San Diego, CA, USA, May 7-9, 2015, Conference Track Proceedings</i> .	760
		761
		762
		763
		764
		765
	Mengxue Yang, Chun Yang, Jiaqi Zhu, Jiafan Li, Jingqi Zhang, Yuyang Li, and Ying Li. 2025a. <a href="#">SLiNT: Structure-aware language model with injection and contrastive training for knowledge graph completion</a> . In <i>Findings of the Association for Computational Linguistics: EMNLP 2025</i> , pages 13658–13671, Suzhou, China. Association for Computational Linguistics.	766
		767
		768
		769
		770
		771
		772
	Rui Yang, Jiahao Zhu, Jianping Man, Hongze Liu, Li Fang, and Yi Zhou. 2025b. <a href="#">GS-KGC: A generative subgraph-based framework for knowledge graph completion with large language models</a> . <i>Inf. Fusion</i> , 117:102868.	773
		774
		775
		776
		777
	Mohammad Yani and Adila Alfa Krisnadhi. 2021. <a href="#">Challenges, techniques, and trends of simple knowledge graph question answering: A survey</a> . <i>Inf.</i> , 12(7):271.	778
		779
		780
	Fuxiang Zhang, Xin Wang, Zhao Li, and Jianxin Li. 2020. <a href="#">Transrhs: A representation learning method for knowledge graphs with relation hierarchical structure</a> . In <i>Proceedings of the Twenty-Ninth International Joint Conference on Artificial Intelligence, IJCAI 2020</i> , pages 2987–2993. ijcai.org.	781
		782
		783
		784
		785
		786
	Richong Zhang, Junpeng Li, Jiajie Mei, and Yongyi Mao. 2018. <a href="#">Scalable instance reconstruction in knowledge bases via relatedness affiliated embedding</a> . In <i>Proceedings of the 2018 World Wide Web Conference on World Wide Web, WWW 2018, Lyon, France, April 23-27, 2018</i> , pages 1185–1194. ACM.	787
		788
		789
		790
		791
		792
	Xue Zhou, Bei Hui, Ilana Zeira, Hao Wu, and Ling Tian. 2023. <a href="#">Dynamic relation learning for link prediction in knowledge hypergraphs</a> . <i>Appl. Intell.</i> , 53(22):26580–26591.	793
		794
		795
		796

## A Theoretical Justification of Graph-CoT Reasoning

### A.1 Path-Level Aggregation vs. Local Hyperedge Encoding

**Setup.** Let  $\mathcal{H} = (\mathcal{V}, \mathcal{R}, \mathcal{T})$  be a knowledge hypergraph. Given a query hyperedge  $e_q = (r; u_1, \dots, u_{i-1}, ?, u_{i+1}, \dots, u_n)$ , HyperCoT first constructs an initial *local* structural state  $h_{e_q}^{(0)} \in \mathbb{R}^d$  using the high-order representation operator in Section 4.1. For brevity, we denote this local representation by  $h_0 := h_{e_q}^{(0)}$ .

HyperCoT then applies the  $L$ -step structural propagation operator described in Section 4.2, producing hyperedge states  $\{h_e^{(l)}\}_{l=0}^L$  in the shared space  $\mathbb{R}^d$ , where  $(l)$  denotes the  $l$ -th propagation step. Let  $\tilde{\mathcal{P}}_L$  be the candidate length- $L$  path space defined in Section 4.2, and let  $\text{TopK}(\tilde{\mathcal{P}}_L)$  return the top- $K$  paths after beam pruning.

For each selected path  $P_k = (e_k^{[0]}, \dots, e_k^{[L]})$ , where  $e_k^{[0]} = e_q$ , its embedding  $h_{P_k}$  is computed by the depth-aware aggregation in Section 4.2. Finally, Graph-CoT is obtained by the path aggregation in Eq. (11).

**Local encoding as a special case.** We show that the proposed Graph-CoT representation strictly generalizes a local hyperedge encoding.

**Proposition 1** (Local encoding as a special case). *Assume that  $g(\cdot)$  contains the identity map on  $\mathbb{R}^d$  and that the aggregation weights can select a single path. Then there exists a configuration of  $(L, K, \{\omega_l^{[k]}\}, \{\gamma_k\})$  such that*

$$h_{\text{Graph}}(e_q) = h_0.$$

*Proof.* Choose  $L = 0$  so that no propagation is applied and the path space contains the single zero-hop path  $P_1 = (e_1^{[0]})$  with  $e_1^{[0]} = e_q$ . By definition,  $h_{P_1} = h_{e_1^{[0]}}^{(0)} = h_{e_q}^{(0)} = h_0$ . Set  $K = 1$ ,  $\gamma_1 = 1$ , and let  $g$  be the identity map. Then  $h_{\text{Graph}}(e_q) = g(h_{P_1}) = h_0$ .  $\square$

**Implication.** Proposition 1 implies that Graph-CoT is at least as expressive as local hyperedge encoding. Allowing  $L > 0$  and  $K > 1$  enables incorporating multi-hop structural dependencies that cannot be captured by local representations alone.

### A.2 Stability Motivation of Top- $K$ Path Aggregation

Aggregating all reachable paths can be undesirable, as weakly supported paths may introduce noisy or conflicting evidence. HyperCoT therefore aggregates only the Top- $K$  structurally reliable paths. We provide a variance-based justification under a standard estimator view.

**Path-level evidence as random variables.** For a fixed candidate entity  $y \in \mathcal{V}$ , treat the evidence contributed by a structural path  $P_k$  as a random variable

$$X_{P_k}(y) = \langle h_{P_k}, h_y^{[0]} \rangle, \quad (18)$$

where  $h_y^{[0]} \in \mathbb{R}^d$  is the structural embedding of entity  $y$  in the shared space, consistent with the initialization in Section 4.2. Randomness may arise from attention estimation, incomplete neighborhoods, and approximate propagation or beam pruning.

Given a subset of paths  $\mathcal{S}$ , define the aggregated evidence estimator as

$$\hat{C}_{\mathcal{S}}(y) = \frac{1}{|\mathcal{S}|} \sum_{P_k \in \mathcal{S}} X_{P_k}(y). \quad (19)$$

**Proposition 2** (Top- $K$  aggregation reduces variance under reliability ordering). *Assume  $\{X_{P_k}(y)\}$  are independent and that  $\text{Var}[X_{P_k}(y)]$  is non-decreasing as path reliability decreases. Let  $\mathcal{S}_K$  be the set of Top- $K$  reliable paths and  $\mathcal{S}_M$  any set of  $M > K$  paths that includes less reliable ones. Then*

$$\text{Var}[\hat{C}_{\mathcal{S}_K}(y)] \leq \text{Var}[\hat{C}_{\mathcal{S}_M}(y)], \quad (20)$$

*up to a constant factor when  $M$  grows by adding higher-variance paths.*

*Proof.* By independence,

$$\text{Var}[\hat{C}_{\mathcal{S}}(y)] = \frac{1}{|\mathcal{S}|^2} \sum_{P_k \in \mathcal{S}} \text{Var}[X_{P_k}(y)]. \quad (21)$$

Under the stated reliability ordering, enlarging  $\mathcal{S}_K$  to  $\mathcal{S}_M$  by adding less reliable (higher-variance) paths increases the average variance term, yielding a larger (or no smaller) estimator variance.  $\square$

**Discussion.** Proposition 2 provides a principled bias–variance perspective: restricting aggregation to Top- $K$  reliable paths suppresses noisy structural evidence while preserving strongly supported constraint compositions. In HyperCoT, the reliability

---

**Algorithm 1:** Attention-Induced Structural Path Extraction

---

**Input:** Query hyperedge  $e_q$ ;  
entity-hyperedge attention weights  $\{\alpha_{v,e}^{(l)}, \beta_{e,v}^{(l)}\}_{l=0}^{L-1}$ ; reasoning depth  $L$ ;  
beam size  $K$

**Output:** Top- $K$  structural paths  $\{P_k\}_{k=1}^K$

Initialize beam  $\mathcal{B}_0 = \{((e_1^{[0]}), 0)\}$  with  $e_1^{[0]} = e_q$ , where each element is a (path, score) pair;

**for**  $l = 0$  **to**  $L - 1$  **do**

    Initialize empty beam  $\mathcal{B}_{l+1}$ ;

**foreach**  $(P_k, s) \in \mathcal{B}_l$  **do**

        Let  $e_k^{[l]}$  be the last hyperedge in path  $P_k$ ;

**foreach**  $e_k^{[l+1]} \in \mathcal{N}_H(e_k^{[l]})$  **do**

            Compute transition score:

$$\pi^{[l]}(e_k^{[l]} \rightarrow e_k^{[l+1]}) = \sum_{v \in e_k^{[l]} \cap e_k^{[l+1]}} \alpha_{v, e_k^{[l]}}^{(l)} \beta_{e_k^{[l+1]}, v}^{(l)}$$

            Add  $(P_k \cup \{e_k^{[l+1]}\}, s +$

$$\log \pi^{[l]}(e_k^{[l]} \rightarrow e_k^{[l+1]}))$$
 to  $\mathcal{B}_{l+1}$ ;

    Keep the top- $K$  elements in  $\mathcal{B}_{l+1}$  ranked by score;

**return**  $\mathcal{B}_L$

---

883 scores defined in Section 4.3 induce the ordering  
884 required by this analysis, making Top- $K$  aggrega-  
885 tion a stability mechanism rather than a heuristic  
886 truncation.

## B Algorithmic Details

### B.1 Attention-Induced Structural Path Extraction

887 This section presents the detailed procedure for  
888 extracting *attention-induced structural paths* de-  
889 scribed in Section 4.2. The algorithm explicitly  
890 follows the multi-hop propagation and path scoring  
891 formulation in the main text.  
892  
893  
894

895 **Remarks.** The algorithm performs a beam search  
896 over hyperedges starting from the query hyperedge  
897  $e_k^{[0]} = e_q$ . At each step  $l$ , transitions between hyper-  
898 edges are induced by the entity-hyperedge at-  
899 tention weights  $\alpha_{v, e_k^{[l]}}^{(l)}$  and  $\beta_{e_k^{[l+1]}, v}^{(l)}$  obtained from  
900 the  $l$ -th propagation step described in Section 4.2.  
901 The algorithm thus provides an explicit procedural  
902 realization of the attention-induced structural paths  
903 used in the main text.

## C Computational Efficiency Analysis

904 We analyze the computational overhead introduced  
905 by HyperCoT beyond a shared language model  
906 backbone. Table 5 reports the structural param-  
907 eter size and relative inference overhead, where  
908 efficiency statistics for GNN-based KGC models  
909 (without language model components) are taken  
910 from prior work under identical experimental set-  
911 tings (Li et al., 2025).  
912

913 Overall, HyperCoT introduces a modest  
914 inference-time overhead (15%–21%) due to ex-  
915 plicit multi-hop structural reasoning. This over-  
916 head is structurally bounded: the additional cost  
917 scales linearly with the reasoning depth  $L$  and the  
918 number of selected paths  $K$ , both fixed to small  
919 constants in practice, and does not depend on the  
920 size of the knowledge hypergraph.

## D Experimental Details and Hyperparameter Analysis

### D.1 Dataset Statistics and Structural Properties

921 We evaluate HyperCoT on three widely used bench-  
922 marks for n-ary knowledge graph completion:  
923 JF17K (Liu et al., 2021), FB-AUTO (Fatemi et al.,  
924 2020), and WikiPeople (Guan et al., 2019). Table 6  
925 summarizes their dataset statistics. Beyond scale,  
926 we emphasize their structural characteristics, which  
927 are critical for assessing multi-hop and structure-  
928 aware reasoning.  
929

930 **JF17K.** JF17K is a large-scale n-ary knowledge  
931 graph derived from Freebase, containing 28,645  
932 entities and 322 relations. Its facts exhibit arities  
933 ranging from 2 to 6, with a substantial portion  
934 of higher-arity relations. As shown in Table 6,  
935 more than 45% of the facts involve arity  $\geq 3$ , mak-  
936 ing JF17K a challenging benchmark that requires  
937 modeling role-dependent interactions and composi-  
938 tional constraints across multiple arguments.  
939

940 **WikiPeople.** WikiPeople is constructed from  
941 Wikipedia tables and infoboxes and represents one  
942 of the largest benchmarks for n-ary reasoning. It  
943 contains 47,765 entities and 707 relations, with ar-  
944 ities ranging from 2 to 9. The dataset is dominated  
945 by binary facts, but still includes a non-trivial num-  
946 ber of ternary and higher-arity instances. This mix-  
947 ture of low- and high-arity facts makes WikiPeople  
948 suitable for evaluating the robustness of models  
949 under heterogeneous structural complexity.  
950  
951

Table 5: Efficiency comparison between hypergraph-based KGC models and HyperCoT. Best results are shown in **bold**, second-best results are underlined.

Model	Structural Parameters (M)			Relative Inference Overhead (%)		
	JF17K	WikiPeople	FB-AUTO	JF17K	WikiPeople	FB-AUTO
PosKHG	14.34	27.53	1.65	–	–	–
HyConvE	12.80	21.44	4.80	–	–	–
ReAIE	14.88	29.61	1.64	–	–	–
HyCubE	<b>1.28</b>	<b>2.24</b>	<b>0.96</b>	–	–	–
HyCubE+	<u>5.77</u>	<u>13.46</u>	<u>1.28</u>	–	–	–
<b>HyperCoT</b>	11.52	19.20	3.84	+18%	+21%	+15%

**FB-AUTO.** FB-AUTO is a domain-specific n-ary knowledge graph in the automotive domain, consisting of 3,388 entities and 8 relations. Although smaller in scale, FB-AUTO exhibits a high proportion of higher-arity facts (arity  $\geq 4$ ), reflecting complex real-world relational structures such as manufacturing, ownership, and production chains. This dataset is structurally sparse and requires leveraging indirect evidence across multiple hops, making it particularly suitable for evaluating explicit structural reasoning and interpretability.

**Structural Implications.** Across all datasets, higher-arity facts account for a significant fraction of the data, highlighting the limitations of methods designed primarily for binary relations. Moreover, the presence of structurally sparse entities and long-tail role combinations motivates the need for path-level reasoning mechanisms such as Graph-CoT, which can aggregate indirect structural evidence beyond local hyperedges.

## D.2 LLM-based Baseline Models and Training Configuration

**LLM-based Baseline Models.** We compare HyperCoT against a diverse set of strong language model baselines, including both open-source and proprietary models, under Fine-tuned and zero-shot settings.

**LLaMA-2-7B** (Touvron et al., 2023) is a 7B-parameter decoder-only language model pretrained on large-scale general-domain corpora and fine-tuned on each benchmark using the same supervision as HyperCoT.

**Mistral-7B-Instruct** (Jiang et al., 2023) is a 7B instruction-tuned language model optimized for following natural language prompts and fine-tuned on the target tasks.

**Qwen-2-7B-chat** (Yang et al., 2024) is a 7B instruction-tuned model from the Qwen2 series

designed for efficient reasoning under limited computational budgets.

**Gemma-2-9B-Instruct** (Google DeepMind, 2024) is an instruction-tuned model from the Gemma-2 series with 9B parameters, focusing on improved reasoning and generation quality.

**GPT-4o-mini** (OpenAI, 2024) is proprietary large language models evaluated in zero-shot settings using task-specific prompts.

**LLaMA-3-8B-Instruct** (Grattafiori et al., 2024) is a fine-tuned baseline sharing the same backbone as HyperCoT but without structure-aware reasoning.

**Implementation Details.** HyperCoT is implemented in PyTorch. The decoder is instantiated with a LLaMA-3-8B-Instruct model and fine-tuned using Low-Rank Adaptation (LoRA) (Hu et al., 2022), while the backbone parameters remain frozen. LoRA is applied with rank  $r = 128$ , scaling factor  $\alpha = 64$ , and dropout rate of 0.1.

Unless otherwise specified, we use  $L = 3$  structural reasoning layers and select the Top- $K = 5$  structural paths for Graph-CoT aggregation. The structural aggregation coefficient  $\eta$  in Eq. 12 controls the contribution of individual structural paths and is fixed to 0.5 across all experiments.

Training is performed using the AdamW optimizer with a learning rate of  $2 \times 10^{-4}$ . Model checkpoints are selected based on validation MRR. All experiments are conducted on up to two NVIDIA H100 GPUs (80GB) under a consistent hardware environment.

## D.3 Sensitivity to Structural Hyperparameters

We analyze the sensitivity of HyperCoT to two key hyperparameters that control structure-aware learning and aggregation: the structural alignment weight  $\lambda$  in the training objective (Section 4.5) and

Table 6: Statistics of the datasets.

Dataset	$ \mathcal{E} $	$ \mathcal{R} $	Arity	#Train	#Valid	#Test	#Arity=2	#Arity=3	#Arity=4	#Arity $\geq$ 5
JF17K	28,645	322	2–6	61,104	15,275	24,568	54,627	34,544	9,509	2,267
WikiPeople	47,765	707	2–9	305,725	38,223	38,281	337,914	25,820	15,188	3,307
FB-AUTO	3,388	8	2,4,5	6,778	2,255	2,180	3,786	–	215	7,212

Table 7: Effect of structural alignment weight  $\lambda$  on MRR.

$\lambda$	JF17K (MRR)	WikiPeople (MRR)	FB-AUTO (MRR)
0.1	0.576	0.437	<b>0.904</b>
0.3	<b>0.599</b>	0.440	0.883
0.5	0.551	<b>0.451</b>	0.870
0.7	0.532	0.427	0.866

Table 8: Effect of path reliability coefficient  $\eta$  on MRR.

$\eta$	JF17K(MRR)	WikiPeople(MRR)	FB-AUTO(MRR)
0.0	0.581	0.438	0.892
0.3	0.593	0.446	0.899
0.5	<b>0.599</b>	<b>0.451</b>	<b>0.904</b>
0.7	0.592	0.443	0.897

the path reliability coefficient  $\eta$  in Graph-CoT aggregation (Eq. 12).

### D.3.1 Sensitivity to Structural Alignment Weight $\lambda$

We first examine the effect of the structural alignment weight  $\lambda$ , which balances entity prediction accuracy and structural regularization. Table 7 reports the MRR of HyperCoT under different  $\lambda$  values across three benchmarks.

Overall, HyperCoT exhibits stable performance over a broad range of  $\lambda$  values, with clear dataset-dependent preferences. On JF17K, moderate alignment weights (e.g.,  $\lambda = 0.3$ ) yield the best performance, suggesting a balanced contribution between entity prediction and structural regularization. On WikiPeople, slightly larger  $\lambda$  values are favored, indicating a stronger reliance on structural alignment under sparse and heterogeneous settings. In contrast, FB-AUTO achieves optimal performance with smaller  $\lambda$ , reflecting its stronger type constraints and more regular relational structure. Across all datasets, performance degrades only when structural regularization is overly emphasized, demonstrating that HyperCoT is robust to moderate variations in  $\lambda$ .

### D.3.2 Sensitivity to Path Reliability Coefficient $\eta$

We further analyze the sensitivity to the path reliability coefficient  $\eta$ , which controls the contribution of structure-aware path reliability in Graph-CoT aggregation (Eq. 12). Table 8 reports the MRR under different  $\eta$  values.

Overall, HyperCoT exhibits stable performance over a broad range of  $\eta$ . Moderate values (e.g.,  $\eta = 0.5$ ) consistently achieve the best or near-best

**Instruction**  
You are given an **incomplete fact** with one missing entity.

**Fact:**  
**Relation** : <RELATION>

**Arguments:**

- <ROLE\_1 > : <ENTITY\_1>
- <ROLE\_2 > : <ENTITY\_2>
- <ROLE\_i > : **[MISSING]**
- ...
- <ROLE\_n > : [ENTITY\_n]

**Candidate Entities:**  
The missing entity must be selected from the following candidates:

- <CANDIDATE\_1>;
- <CANDIDATE\_2>;
- <CANDIDATE\_3>;
- ...

**Task:**  
Select the entity that **best completes** the fact. Output only the entity name.

Figure 5: Prompt template for an incomplete  $n$ -ary fact.

performance across datasets. Very small  $\eta$  underweights structural reliability, while overly large  $\eta$  overemphasizes path consistency and slightly degrades performance. Unless otherwise specified, we set  $\eta = 0.5$  in all experiments.

## E Prompt Template

To interface structural reasoning with language-based scoring, HyperCoT linearizes each query hyperedge into a structured natural language prompt. The prompt explicitly specifies the incomplete  $n$ -ary fact and a constrained candidate entity set, while structural reasoning results (Graph-CoT) are *not* provided as textual input.

**Prompt Format.** Given a query hyperedge  $e_q = (r; u_1, \dots, u_{i-1}, ?, u_{i+1}, \dots, u_n)$ , the prompt is constructed as shown in Fig. 5.

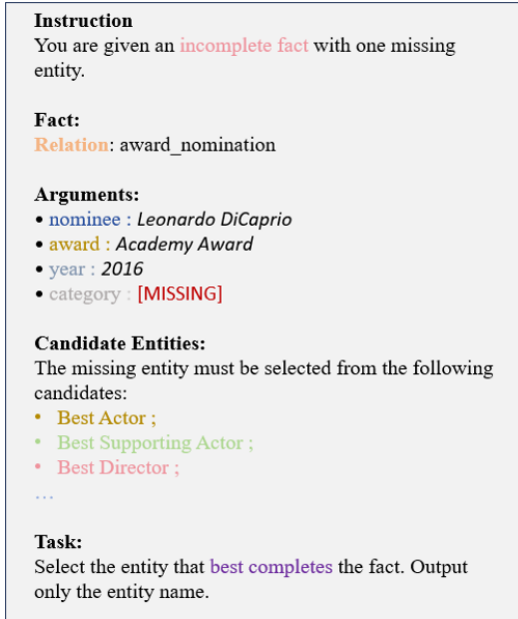


Figure 6: Concrete prompt example used for candidate-constrained decoding.

**Prompt Example.** An instantiated example of the prompt is shown in Fig. 6.

## F Alignment Loss Formulation

**Alignment Loss.** The alignment loss  $\mathcal{L}_{\text{align}}$  enforces consistency between the Graphical Chain-of-Thought representation and the ground-truth entity in the shared structural embedding space.

Formally, given a query hyperedge  $e_q$  and its ground-truth entity  $v^+$ , the alignment loss is defined as:

$$\mathcal{L}_{\text{align}} = -\log \frac{\exp(\cos(h_{\text{Graph}}(e_q), h_{v^+}))}{\sum_{v \in \mathcal{C}(e_q)} \exp(\cos(h_{\text{Graph}}(e_q), h_v))}, \quad (22)$$

where  $h_{\text{Graph}}(e_q)$  denotes the Graph-CoT representation,  $h_v$  is the structural embedding of entity  $v$ , and  $\mathcal{C}(e_q)$  is the candidate entity set. This formulation encourages the aggregated structural evidence to be aligned with the correct entity while discriminating against competing candidates.

## G Case Studies and Interpretability Analysis

### G.1 Case Studies Across Datasets

We present representative case studies from three datasets with distinct structural characteristics, including both successful and failure cases. For each dataset, we analyze an incomplete query hyperedge together with the top-ranked structural paths

induced by HyperCoT. For clarity, we display the top-3 paths among the top-5 used during inference. Concrete entity names are used for readability.

#### G.1.1 Case Study on FB-AUTO (Successful Case)

This case involves a high-arity automotive manufacturing relation with one missing argument, where the goal is to identify the manufacturing plant of a specific vehicle configuration. As shown in Table 9, HyperCoT retrieves multiple structural paths that connect the vehicle model to candidate plants through complementary production-related relations. While each path captures only partial evidence, their aggregation jointly enforces consistency across model, brand, engine, and market information. Consequently, HyperCoT correctly ranks *Mississippi Plant* as the most plausible completion.

#### G.1.2 Case Study on JF17K (Failure Case)

We next present a failure case from JF17K that highlights the limitation of structure-guided reasoning under structural ambiguity. The query corresponds to the relation `cvg.musical_game_song_relationship`, where the task is to predict the artist of a game soundtrack given the game and song. As shown in Table 10, the extracted structural paths connect *Final Fantasy VII* and *One-Winged Angel* to multiple candidate artists via contribution and group membership relations. However, these paths provide comparable structural support for different artists and fail to impose a role-specific constraint that uniquely identifies the ground-truth answer. As a result, the aggregated Graph-CoT ranks *Masashi Hamauzu* above the correct artist *Nobuo Uematsu*.

#### G.1.3 Case Study on WikiPeople (Successful Case)

This case is drawn from the WikiPeople dataset and illustrates a qualifier-aware role completion scenario with temporal constraints. The query requires predicting a position held by a person during a specific time interval. As shown in Table 11, HyperCoT extracts multiple query-conditioned structural paths that explicitly associate candidate positions with their corresponding start and end times. Only the paths corresponding to *President of the United States* satisfy the temporal constraints between 2009 and 2017. By aggregating these paths, Hyper-

Table 9: Graph-CoT reasoning example for a successful case on FB-AUTO. Entity identifiers are mapped to surface names for readability.

<b>Incomplete Query Hyperedge</b>	(model; <i>Toyota Corolla 2019, 2.0L Engine, Toyota, ?, North America</i> )
<b>Top-3 Structural Paths</b>	<p><b>Path 1 (direct model–plant evidence):</b>          (model; <i>Toyota Corolla 2019, 2.0L Engine, Toyota, ?, North America</i>)          → (manufacturing_plant_model_relationship; <i>Toyota Corolla 2019, Mississippi Plant</i>)</p> <p><b>Path 2 (brand-mediated structural evidence):</b>          (model; <i>Toyota Corolla 2019, 2.0L Engine, Toyota, ?, North America</i>)          → (make; <i>Toyota Corolla 2019, Toyota</i>)          → (manufacturing_plant_model_relationship; <i>Toyota, Mississippi Plant</i>)</p> <p><b>Path 3 (engine-consistent production evidence):</b>          (model; <i>Toyota Corolla 2019, 2.0L Engine, Toyota, ?, North America</i>)          → (engine; <i>Toyota Corolla 2019, 2.0L Engine</i>)          → (manufacturing_plant_engine_relationship; <i>2.0L Engine, Mississippi Plant</i>)</p>

Table 10: Graph-CoT reasoning example for a failure case on JF17K. Entity identifiers are mapped to surface names for readability.

<b>Incomplete Query Hyperedge</b>	(cvg.musical_game_song_relationship; <i>Final Fantasy VII, ?, One-Winged Angel</i> )
<b>Top-3 Structural Paths</b>	<p><b>Path 1 (direct contribution evidence):</b>          (cvg.musical_game_song_relationship; <i>Final Fantasy VII, ?, One-Winged Angel</i>)          → (music.recording_contribution; <i>One-Winged Angel, Masashi Hamauzu</i>)</p> <p><b>Path 2 (group-mediated participation evidence):</b>          (cvg.musical_game_song_relationship; <i>Final Fantasy VII, ?, One-Winged Angel</i>)          → (music.recording_contribution; <i>One-Winged Angel, Nobuo Uematsu</i>)          → (music.group_membership; <i>Nobuo Uematsu, Square Enix Music</i>)</p> <p><b>Path 3 (game-level performance evidence):</b>          (cvg.musical_game_song_relationship; <i>Final Fantasy VII, ?, One-Winged Angel</i>)          → (cvg.game_performance; <i>Square Enix Music, Final Fantasy VII</i>)</p>

1153 CoT suppresses temporally incompatible roles and  
 1154 correctly identifies the ground-truth position.

## 1155 G.2 Discussion: Interpretability of 1156 Graph-CoT

1157 Across all datasets, these case studies demonstrate  
 1158 that Graph-CoT provides explicit and verifiable  
 1159 structural evidence supporting the model’s predic-  
 1160 tions. By exposing ranked multi-hop reasoning  
 1161 traces, HyperCoT enables transparent analysis of  
 1162 how structural information is utilized, in contrast to  
 1163 embedding-based or purely generative approaches  
 1164 that do not offer explicit reasoning paths.

Table 11: Graph-CoT reasoning example for a successful case on WikiPeople. Entity identifiers are mapped to surface names for readability.

<b>Incomplete Query Hyperedge</b>	(P39 / P580 / P582; <i>Barack Obama</i> , ?, 2009, 2017)
<b>Top-3 Structural Paths</b>	<p><b>Path 1 (position–time consistency evidence):</b>  (P39 / P580 / P582; <i>Barack Obama</i>, ?, 2009, 2017)  → (P39; <i>Barack Obama</i>, <i>President of the United States</i>)  → (P580; <i>President of the United States</i>, 2009)  → (P582; <i>President of the United States</i>, 2017)</p> <p><b>Path 2 (citizenship-constrained role evidence):</b>  (P39 / P580 / P582; <i>Barack Obama</i>, ?, 2009, 2017)  → (P27; <i>Barack Obama</i>, <i>United States</i>)  → (P39; <i>United States</i>, <i>President of the United States</i>)</p> <p><b>Path 3 (temporal conflict evidence for an alternative role):</b>  (P39 / P580 / P582; <i>Barack Obama</i>, ?, 2009, 2017)  → (P39; <i>Barack Obama</i>, <i>Senator of the United States</i>)  → (P580; <i>Senator of the United States</i>, 2005)  → (P582; <i>Senator of the United States</i>, 2008)</p>